EPI-SIDE-DOWN MOUNTING OF INTERBAND CASCADE LASERS FOR ARMY APPLICATIONS

M. S. Tobin, C. J. Monroy, K. A. Olver, R. L. Tober
Army Research Laboratory
Adelphi, MD, 20783-1138

J. L. Bradshaw, J. D. Bruno and F. J. Towner,
Maxion Technologies, Inc.
Hyattsville, MD 20782-2055

ABSTRACT

The interband cascade laser, based on the type II energy band alignment in the InAs/GaSb material system, has great potential to meet the power and the wall plug efficiency requirements of many Army applications. However, the development of interband cascade lasers has lagged the development of InP-based quantum cascade lasers. These latter devices have recently exhibited high power, room temperature, cw operation at 3.8 µm and at longer wavelengths. Only a few groups are working on the interband cascade lasers, and relatively modest progress has been made in advancing their high-temperature performance. In this paper, we describe our efforts to improve the high-temperature performance of these sources using epi-side-down mounting.

1. INTRODUCTION

High-performance semiconductor lasers operating in the mid-wave (3-5 µm) and long-wave (8-12 µm) infrared (IR) spectral regions are attractive sources for use in a wide range of military and civilian applications. In order to meet the needs of a lighter, more deployable, and yet lethal and survivable Army, non-cryogenically cooled lasers are required that can operate in continuous wave (cw) or quasi-cw mode at ambient temperatures or at temperatures accessible to thermoelectric coolers (T > ~ -30C).

There are several types of semiconductor lasers that operate in the mid-wave and the long-wave region of the infrared. These include lead-salt lasers (Shi et al. 1995), III-V-based antimonide interband lasers (Choi et al. 1995), type-II-transition-based lasers (Meyer J.R. 1995,

Malin et al. 1996), the interband cascade lasers (ICLs) (Lin, et al. 1997), and quantum cascade lasers (QCLs) (Gmachl et al. 2001). The QCLs are presently the performance leaders in this group in terms of high power and high temperature operation. The QCLs are unipolar semiconductor injection lasers that rely on transitions between conduction subbands in a multiple quantum well heterostructure. Depending on the design and thickness of the quantum wells, QCLs can cover a wide wavelength range from the mid-IR to the terahertz. These lasers make use of a cascade process in which multiple photons can be generated per electron, as the electron remains inside the conduction band throughout its traversal of the active region.

Excellent progress has been made in the high temperature and high power performance of the InP-based unipolar QCLs in the mid- and long-wave IR regions; cw operation at the 150-mW level has been achieved at ambient and greater temperatures at various wavelengths from ~3.8 µm to ~9.5µm (Yu and Evans et al. 2006; Evans et al. 2004; Evans et al. 2006; Yu and Slivken et al. 2006). Much of the recent improvement in high power and temperature operation is attributed to better heat management through the development of effective epi-side-down bondings using AlN (Tsekoun et al. 2006) and diamond submounts (Yu and Evans et al. 2006). Notwithstanding their superior high temperature performance characteristics, QCLs suffer from very low wall plug efficiencies (WPEs) near room temperature with the highest reported WPEs just under a few percent. Moreover, it is unlikely that much improvement can be made to the WPEs of QCLs given their very low radiative efficiencies. This represents a serious issue for many Army applications, and this is where ICLs have significant potential.

The present work is concerned with the heat management of Type II Interband Cascade Lasers (ICLs)

Report Documentation Page	*Form Approved* *OMB No. 0704-0188*

Public reporting burden for the collection of information is estimated to average 1 hour per response, including the time for reviewing instructions, searching existing data sources, gathering and maintaining the data needed, and completing and reviewing the collection of information. Send comments regarding this burden estimate or any other aspect of this collection of information, including suggestions for reducing this burden, to Washington Headquarters Services, Directorate for Information Operations and Reports, 1215 Jefferson Davis Highway, Suite 1204, Arlington VA 22202-4302. Respondents should be aware that notwithstanding any other provision of law, no person shall be subject to a penalty for failing to comply with a collection of information if it does not display a currently valid OMB control number.

1. REPORT DATE **01 NOV 2006**	2. REPORT TYPE **N/A**	3. DATES COVERED **-**	
4. TITLE AND SUBTITLE **Epi-Side-Down Mounting Of Interband Cascade Lasers For Army Applications**		5a. CONTRACT NUMBER	
		5b. GRANT NUMBER	
		5c. PROGRAM ELEMENT NUMBER	
6. AUTHOR(S)		5d. PROJECT NUMBER	
		5e. TASK NUMBER	
		5f. WORK UNIT NUMBER	
7. PERFORMING ORGANIZATION NAME(S) AND ADDRESS(ES) **Army Research Laboratory Adelphi, MD, 20783-1138**		8. PERFORMING ORGANIZATION REPORT NUMBER	
9. SPONSORING/MONITORING AGENCY NAME(S) AND ADDRESS(ES)		10. SPONSOR/MONITOR'S ACRONYM(S)	
		11. SPONSOR/MONITOR'S REPORT NUMBER(S)	
12. DISTRIBUTION/AVAILABILITY STATEMENT **Approved for public release, distribution unlimited**			
13. SUPPLEMENTARY NOTES **See also ADM002075., The original document contains color images.**			
14. ABSTRACT			
15. SUBJECT TERMS			

16. SECURITY CLASSIFICATION OF:			17. LIMITATION OF ABSTRACT **UU**	18. NUMBER OF PAGES **7**	19a. NAME OF RESPONSIBLE PERSON
a. REPORT **unclassified**	b. ABSTRACT **unclassified**	c. THIS PAGE **unclassified**			

Standard Form 298 (Rev. 8-98)
Prescribed by ANSI Std Z39-18

based on InAs-InGaSb quantum wells (see e.g., Bruno et al. 2005). These lasers bear some similarities to the QCLs, in particular active and injection regions are stacked in series, so that the lasers retain the principal advantage of electron recycling. However, unlike the QCL, the ICL relies on the cascading of interband optical transitions as opposed to intersubband optical transitions. This characteristic eliminates the fast optical phonon relaxation of the upper laser level and consequently, leads to much higher radiative efficiencies and significantly reduced threshold currents compared with the QCLs. The ICLs have been demonstrated to have very high cw wall-plug efficiencies (>32%). Another advantage of the ICLs is that they are not constrained by optical selection rules to edge-emitting configurations; they can be used in a surface-emitting configuration like near-IR interband lasers. Surface emitting LEDs have already been demonstrated with IC-based structures, (Das et al. 2005), and vertical cavity surface emitting lasers are also possible with this system. One disadvantage of the ICLs is that they are based on the antimonide material system, which is not as well understood compared with the InP system. Although great progress has been made on the ICLs since their conception, development is not as advanced as for the QCLs, and cw room temperature operation has not yet been achieved.

2. HIGH TEMPERATURE ISSUES

Calculations have predicted that ICLs should be capable of operating under cw conditions up to room temperature with high output powers (Vurgaftman et al. 1997); however, to date only pulsed operation at and above room temperature has been achieved. Significant issues limit the high-temperature performance of ICLs. These include the rapid increase of non-radiative processes with increasing active-region temperature (e. g., Auger processes) and the large accumulation of heat in the laser's active region at increased operating temperatures. These issues are being addressed through improved laser design and fabrication techniques. Improvements in device processing techniques to reduce thermal resistance for epi-side-up configurations has led to cw operation up to 221.4K at λ=3.6μm for a 7-μm wide, 2-mm long mesa device (Bradshaw et al. 2004, private communication 2006). The maximum cw operating temperature for ICLs reported to date has been 237K (Yang et al. 2005), with pulsed lasing to 350K and spectral output in the 3.0-3.3-μm region. This device was a 12 cascaded stage structure processed into mesa-stripe lasers without facet coatings and mounted epi-side-up onto a Cu block. The extracted specific thermal resistance was ~10 Kcm^2/kW near 237K. The success of

devices from this particular sample design/growth was in part attributed to a relatively thick bottom cladding layer with resulting reduced light leakage to the substrate. Whereas improved laser design can lead to improvements in high temperature performance, this paper addresses heat management in these devices, and more specifically, the critical issues associated with the attachment of the laser die to the heat sink.

Heat removal is an important aspect in the performance of all semiconductor lasers, and it is especially critical with ICLs, which are fabricated from materials that have relatively low thermal conductivities. Table 1 shows the thermal conductivity (κ) and coefficient of thermal expansion (CTE) of some common materials used for semiconductor lasers. (Reported values vary depending on source and measurement methods.) The ICLs are grown on GaSb substrates, which have a thermal conductivity of approximately 33 W/m-K compared with 68 W/m-K for InP. Moreover, the κ of the InAs/AlSb superlattice cladding material generally used in these devices is probably less than ~ 3.6 W/m-K. Even though the claddings are much thinner (~ 2 μm) than the thinned substrate used in devices (~ 100 μm), this very small cladding layer κ is significant - making the temperature drop across the cladding layer an important contribution to the overall device thermal resistance.

Table 1. Thermal conductivity and coefficient of thermal expansion of some materials useful for construction of infrared semiconductor lasers.

Material	Therm. Cond. κ (W/m-K)	CTE (10^{-6} K^{-1})
InP	70/68	4.5
GaAs	~ 44	5.9
GaSb	~33 (Bruno 2005)	7.75
InAs/AlSb cladding layer	< 3.6 (Bruno 2005)	
BeO	250 /290	6, 7.6, 9.0
Cu	393	17
SiC	120	4
AlN	230 (high grade –Tsekoun 2006)	4.5, 4.3
Indium	83.7	24.8@ 20C

Epi-side-down mounting of semiconductor lasers has long been used to reduce their thermal resistances and improve their high temperature and high power performance. When mounted in this configuration, the device's active region is only microns away from the heat sink material, and a good thermal bond between the

device ridge and an effective heat spreader material can have a very significant performance payoff. This should be particularly true for the case of ICLs because of the low κ's described above. However, effective epi-side-down mounting is much more challenging than epi-side-up mounting; now the active region is only microns away from the area where molten solder will flow. Soldering must be precise, and the laser facet and edges of the laser die cannot come into contact with the solder as this would short out the device and/or ruin the facet. Additionally, ideally the laser should not overhang the submount by more than a few microns since, in such a case, a hot spot may form leading to device failure. Also, the laser die cannot be much shorter than the submount length, since in this case, clipping of the output beam will occur. Finally, the heat sink must have a good κ and a CTE that matches that of the GaSb substrate so that built-in stresses are tolerable.

3. THERMAL CHARACTERIZATION

It has been found for most diode lasers, including ICLs, that under short pulsed, low duty cycle excitation, the threshold current empirically depends exponentially on temperature as

$$I_{th} = I_o \exp (T_a/T_o) \qquad (1)$$

where T_o and I_o are fitting parameters; T_o is called the characteristic temperature, and T_a is the active region temperature. For many diode lasers, at cryogenic temperatures, where the threshold currents and resulting input powers are relatively low, the cw threshold currents also follow the exponential expression to a very good approximation. At higher temperatures, it is observed that the cw current thresholds deviate significantly from this exponential curve and are greater than what would be predicted by it. T_a can be expressed in terms of the heat sink temperature T_h by

$$T_a = T_h + R_{th}IV \qquad (2)$$

where R_{th} is defined as the device thermal resistance, and V and I are the device's cw voltage and current, respectively, assuming that all the power goes into heat. These expressions can be used to determine the maximum heat sink temperature at which the laser will operate under cw conditions; this temperature is given by

$$T_h(max) = T_o \left(\ln(T_o/R_{sp}V_{th}J_o)-1 \right) \qquad (3)$$

where V_{th} is the threshold voltage across the device at the maximum cw operating temperature, and R_{sp} is the specific thermal resistance of the device defined by the product of R_{th} times A, where A is the device's active

region area: the cavity length times the mesa width, and J_o is the current density parameter and equals Io divided by the active region area.

4. EXPERIMENT

The lasers are grown by molecular beam epitaxy, beginning with an n-type doped InAs/AlSb strained layer superlattice (SLS), which acts as an optical cladding layer (~2-3 μm thick). This is followed by the cascaded active and injection regions (typically ~ 1.4-μm thick), another n-type doped InAs/AlSb SLS (>~1.4-μm thick) cladding region, and finally an n+InAs contact layer. The devices are then processed by etching. Insulating layers and metal contacts are deposited as necessary, and the lasers are cleaved to form parallel facets; the substrate has been thinned down to about 120 μm prior to cleaving. Finally the lasers are ready for mounting. For our initial efforts, we used BeO as a submount, because of the good CTE match to the GaSb as is shown in Table 1. Epi-side-down mounting of the ICLs is performed by flip-chip hybridization using indium as the interconnect solder. Both the laser and the BeO fan-out are patterned with indium stripes. The BeO fan-out is first soldered to a copper block using an indium preform. Next, the two individual parts are placed into the Hybridization Flip Chip Bonder (schematic shown in Fig. 1), which is used to hybridize the ICL epi-side-down onto the BeO/Cu submount. Alignment is achieved by placing the laser and BeO fan-out on the top and bottom chucks and, using the camera system in the bonder, aligning the two
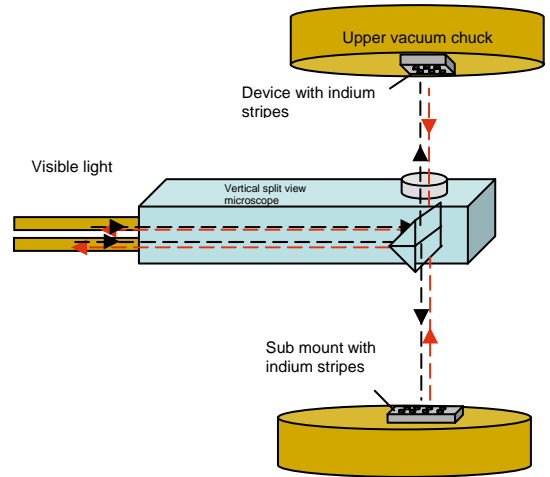

Fig. 1. Alignment of device and submount using a split view microscope and camera system.

parts in the x and y direction as well as correcting for parallelism between the laser die and the sub mount. The camera system in the flip chip bonder is depicted in

Fig.1. The lower chuck assembly can correct for X and Y, rotation, and planarity using the split view microscope. The camera system is removed, and the bottom chuck is raised to the top chuck, which brings the laser bar and the BeO/Cu submount together. Specific amounts of heat and pressure are used to attach (solder) the laser bar to the BeO fan-out. Constant pressure is applied to the bonded device until room temperature is reached before releasing the top and bottom chuck vacuum. Fig. 2 shows a diagram of the laser and the BeO/Cu submount hybridization device. The bonded device is removed from the flip chip bonder, and wires are bonded to each device for testing. Fig. 3 shows an image of the final packaged array. The device is then mounted on a cold finger and placed inside a temperature-controlled cryostat with calcium fluoride windows. Light output – Current- Voltage (L-I-V)
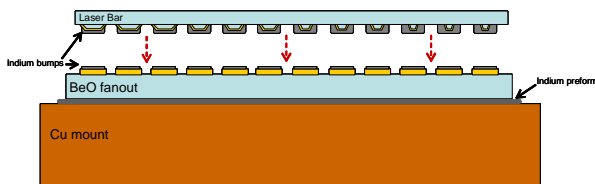

Fig. 2. Diagram of the laser array and BeO/Cu submount hybridization device.

Fig. 3. Image of a completed epi-side-down IC laser array.

characterization curves were taken over a broad range of temperatures from the coldest 78K to the highest temperature that the laser would operate.

.

5. RESULTS

We have produced epi-side-down mounted lasers from several different material growths. M271 was a highly successful growth, as indicated by the good performance of previously tested epi-side-up lasers, and

was selected for the laser material for this series of epi-side-down tests. The first tests were successful in that all of the devices on the resultant M271 epi-side-down array
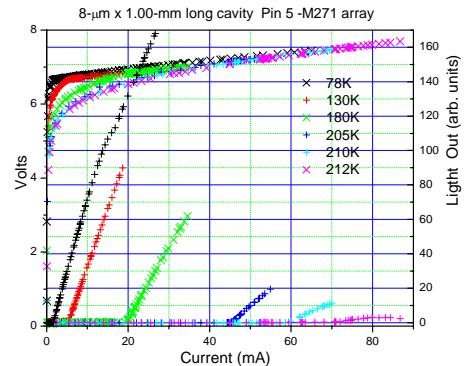

Fig. 4. L-I-V- characteristics from an 8-mm-wide x 1.00–mm-long device 5 of the M271 array under cw contditions at several heat sink
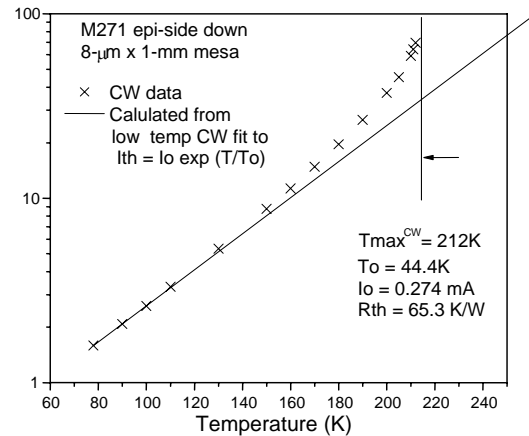

Fig. 5. Threshold current vs heatsink temperature for 8-μm device of M271.
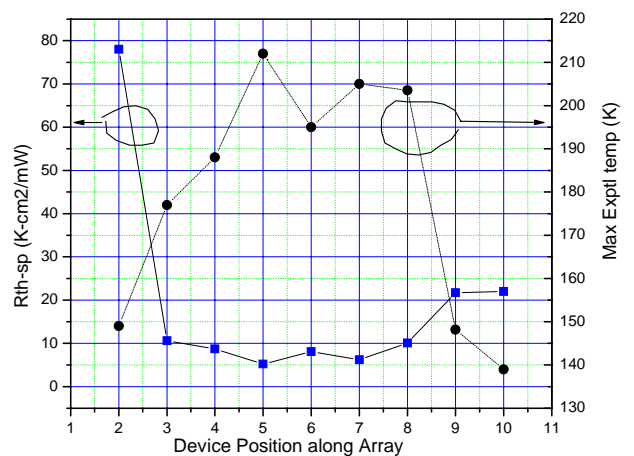

Fig. 6. Specific thermal resistance (left axis) and maximum experimental temperature

were vital and survived multiple cryogenic to room temperature recyclings. Fig. 4 shows an L-I-V curve for device 5 of the array. The results shown are limited to relatively few temperatures in order to simplify the graph. Fig. 5 summarizes the results of current threshold as a function of the temperature for device 5. The four lowest temperatures (80 K to 110K) were used to determine Io and To. It can be seen from the semilog plot, where an exponential gives a straight line, that the current thresholds at the lowest temperature give an excellent linear fit. Similar curves were obtained from all of the other devices on the array and are reported in Table 2. The calculated thermal resistance, specific

shadings of two indium layers is attributed to the difference in depth of the two layers, which is required to allow for cleaving of the laser bar. This image shows the problem of voids that occur, particularly under the isolation trenches. Fig. 8 shows SEM images of each of the individual lasers in the M271 array. It is evident from the images that the devices nos. 2, 9, and 10 have very poor physical contact to the indium layers. These results for this laser bar are likely related to the "smile" of the bar, an effect that often plagues laser arrays. Smile refers to the separation between the lasers and the sub mount near the edges (center) of the laser bar caused by a slight positive (negative) curvature of the laser bar resulting

Table 2. Results for Array M271.

M271 PIN #	Mesa Width (μm)	Io (mA)	To (K)	R th (K/W)	Specific Rth (K-cm2/mW)	T cutoff (K)EXPTL	T cutoff (K) CALC	Δ Tcalc-Texpt
2	4	0.270	43.0	223	78	149	154	5
3	4	0.359	52.6	264	10.6	177	177	0
4	8	0.255	43.0	110	8.7	188	190	1.7
5	8	0.274	44.4	65.3	5.2	212	213	1.4
6	15	0.295	40.9	54.3	8.1	195	200	6
7	15	0.297	40.6	41.4	6.2	205	209	3.2
8	15	0.265	38.8	35.7	10.1	203.5	208	4.2
9	35	0.398	35.5	62.0	21.7	148.2	155	7.7
10	35	0.354	33.2	63.6	22	139	146	7

thermal resistance, experimentally determined maximum cw temperature, and calculated maximum cw temperature are listed. One interesting aspect of the data is that the highest operating temperature and lowest specific thermal resistance are from those devices that are located near the middle of the laser bar. This is summarized in Fig. 6, where the specific thermal resistance is shown on the left vertical axis and the experimental cutoff temperature is shown on the right hand side of the graph.

Scanning electron microscope (SEM) images of the devices were made in an attempt to understand these results. Figure 7 shows a SEM in the backscattered electron imaging mode (BEI mode) for a typical epi-side-down laser with double isolation trenches. Shown are the silicon nitride and gold that are used in the processing of the mesa devices followed by the evaporated indium that joins the indium on the BeO submount for the hybridizing. The difference in the

from built-in stresses in the epi-material. We have made recent progress in minimizing the smile.
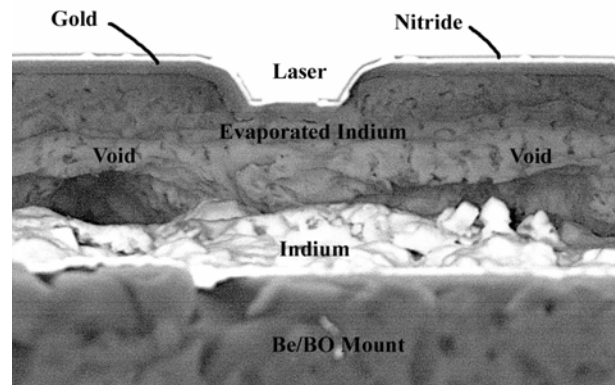

Fig. 7. SEM (BEI) of a laser device mounted epi-side down demonstrating the occurrence of voids in the indium.

Pin#2 4-µm
T_{max} =149K

Pin#3 4-µm
T_{max} =177K

Pin#4 8-µm
T_{max} =212K

Pin#5 8-µm
T_{max} =212K

Pin#6 15-µm
T_{max} =195K

Pin #7 15-µm
T_{max} =205K

Pin #8 15-µm
T_{max} =203.5K

Pin #9 35-µm
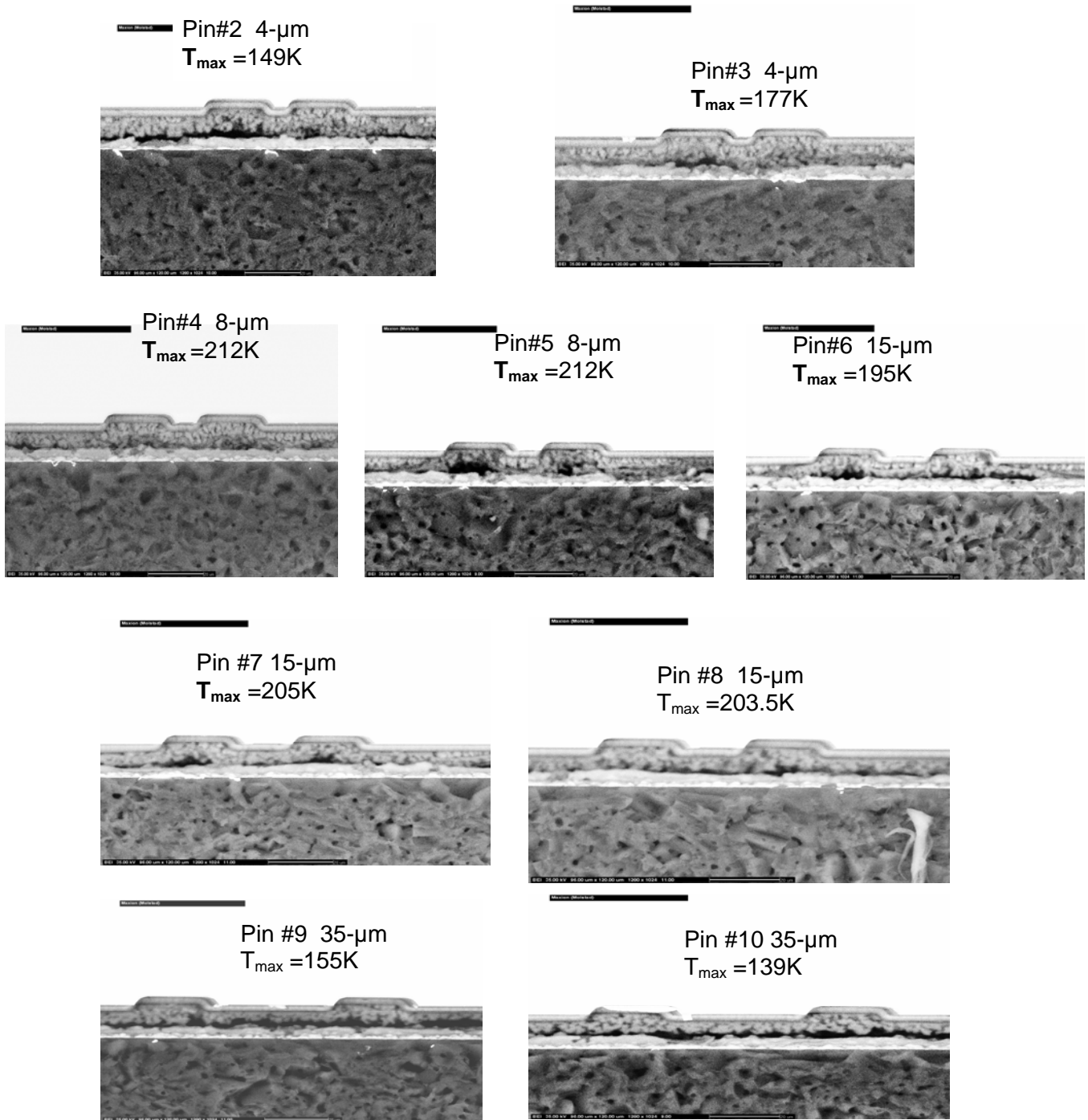T_{max} =155K

Pin #10 35-µm
T_{max} =139K

Fig. 8 Scanning electron microscope images in backscattered electron imaging (BEI) mode for the individual devices of array M271.

However, the voids that occur, particularly under the isolation trenches, remain a problem. Recently we have produced new masks for use in processing the arrays that will allow us to first planarize the lasers by refilling the isolation trenches with electro-plated gold. This should help to eliminate the voids that significantly increase the device thermal resistance. We are also investigating the use of diamond impregnated materials as heat sinks and some alternate bonding methods, and will report on these efforts as well.

SUMMARY

Although ICLs have potential for cw room temperature operation, the best results for an epi-side up laser have been in the 214-240K regions. We are developing methods for epi-side down mounting to remove the heat from the active region. Although we have results that are essentially equivalent to the epi-side-up for the same material growth devices and have produced reliable and robust devices, we have not yet improved their temperature performance. We have identified the problematic issues and are in the process of producing improved devices for testing.

REFERENCES

Shi Z., M. Tacke, A. Lambrecht, and H. Böttner, 1995: Midinfrared lead salt multi-quantum-well diode lasers with 282K operation, *Appl. Phys. Lett.* **66**, 2537-2539.

Choi H.K., G.W. Turner, and H.Q. Le, 1995: InAsSb/InAlAs Strained Quantum-well Lasers emitting at 4.5- μm: *Appl. Phys. Lett.* **66**, 3543-3547.

Meyer J.R., C.A. Hoffman, F.J. Bartoli, and L.R. Ram-Mohan, 1996: Type-II Quantum-Well Lasers for the Mid-wavelength Infrared, *Appl. Phys. Lett.* **67**, 757-759.

Malin, J.I., J.R. Meyer, C.L. Felix, J.R. Lindle, L. Goldberg, C.A. Hoffman, F.J. Bartoli, C.-H. Lin, P.C. Chang, S.J. Murry, R.Q. Yang, and S.-S. Pei, 1996: Type II Mid-Infrared Quantum Well Lasers, *Appl. Phys. Lett.*, **68**, 2976-2978.

Lin, C-H, R.Q. Yang, D Zhang, S. J. Murry, S.S. Pei, A.A. Allerman, and S.R. Kurtz, 1997: Type-II Intraband Quantum Cascade Laser at 3.8 μm, Electron. Lett., **33**, 598-597.

Gmachl, C., F. Capasso, D.L. Sivco, and A.Y. Cho, 2001: Recent Progress in Quantum Cascade Lasers and Applications, *Rep. Prog. Phys.,* **64**, 1533-1601.

Yu J.S., A. Evans, S. Slivken, S.R. Darvish, and M. Razeghi, 2006: Temperature Dependent Characteristics of λ∼3.8μm Room Temperature Continuous-wave Quantum-Cascade Lasers, *Appl. Phys. Lett.*, **88**, 2511189/1-3/.

Evans, C.A, J. S. Yu. S. Slivken, and M. Razeghi, 2004: Continuous-wave Operation of λ∼4.8μm Quantum-Cascade Laser at Room Temperature, *Appl. Phys. Lett.*, **85**, 2166-2168.

Evans, A., J. Nguyen, S. Slivken, J.S. Yu, S.R. Darvish, and M. Razeghi, 2006: Quantum-Cascade Lasers Operating in Continuous-wave above 90 °C at λ∼5.25 μm , *Appl. Phys. Lett.*, **88**, 051105/1-3/.

Yu J.S., S. Slivken A. Evans, S.R. Darvish, J. Nguyen, and M. Razeghi, 2006: High Power λ∼9.5 μm Quantum-Cascade Lasers Operating above Room Temperature in Continuous-Wave Mode, *Appl. Phys. Lett.*, **88**, 091113/1-3/.

Tsekoun , A., R.Go, M. Pushkarsky, M. Razeghi, and C.K.N, Patel, 2006: Improved Performance of Quantum Cascade Lasers through a Scalable, Manufacturable Epitaxial-side-down Mounting Process. *Proc. Nat. Acad. Sci.*, **103**, 4831-4835.

Bruno, J. D., J. L. Bradshaw, N.P. Breznay, J.G. Gomez, R.L. Tober, M.S. Tobin, and F.J. Towner, 2005: Interband Cascade Lasers, Progress and Outlet, *SPIE,* **5617**, 233 -248 .

Das N.C., K. Olver, F. Towner, G. Simonis, and H. Shen, 2005: Infrared (3.8 μm) Interband Cascade Light-emitting Diode Array with Record High Efficiency, *Appl. Phys. Lett.*, **87**, 041105/1-3/.

Vurgaftman I., J.R. Meyer, and L.R. Ram-Mohan, 1997: High Power/Low-Threshold Type_II Interband Cascade Mid-IR Laser- Design and Modeling, *IEEE Photon. Tech. Lett.*, **9**, 170-172.

Bradshaw J.L., N.P. Breznay, J.D. Bruno, J.M. Gomes, J.T. Pham, F.J. Towner, D.E. Wortman, R.L. Tober, C.J. Monroy, and K.A. Olver, 2004,: Recent Progress in the Development of type II Interband Cascade Lasers, *Physica E*, **20**, 479-485.

Yang R.Q., C.J. Hill, and B.H. Yang, 2005: High-temperature and Low-threshold Midinfrared Interband Cascade Lasers, *Appl. Phys. Lett.*, **87**, 151109/1-3/.